

Synthesis of hydrogen-carbon monoxide fuel from methane-carbon dioxide mixed gases

Soichiro SAMEISHIMA, Yoshihiro HIRATA,[†] Kosuke HAMASAKI,* Hironori OHSHIGE and Naoki MATSUNAGA*

Department of Advanced Nanostructured Materials Science and Technology, Kagoshima University, 1-21-40, Korimoto, Kagoshima 890-0065

*Department of Applied Chemistry and Chemical Engineering, Kagoshima University, 1-21-40, Korimoto, Kagoshima 890-0065

Thermal decomposition of methane ($\text{CH}_4 \rightarrow \text{C} + 2\text{H}_2$) needed a high temperature above 900°C and only 15% of methane decomposed at 1000°C . On the other hand, 90% of methane decomposed to form H_2 and C at $700\text{--}900^\circ\text{C}$ by passing through the 70 vol% Al_2O_3 –30 vol% Ni porous compact. When 50% CH_4 –50% CO_2 mixed gases were passed through the porous compact with Ni , 55% H_2 –45% CO fuel was produced at $700\text{--}900^\circ\text{C}$ ($\text{CH}_4 + \text{CO}_2 \rightarrow 2\text{H}_2 + 2\text{CO}$). In a high temperature range from 700 to 900°C , the reforming rate of CH_4 with CO_2 became higher than the pyrolysis rate of CH_4 . The above results were well explained by the thermodynamic calculation along the distance from the surface of $\text{Ni-Al}_2\text{O}_3$ compact against the inlet gas.

©2009 The Ceramic Society of Japan. All rights reserved.

Key-words : Methane, Carbon dioxide, Hydrogen, Carbon monoxide, Nickel

[Received November 5, 2008; Accepted February 19, 2009]

1. Introduction

Biogas produced from excrement of domestic animals contains 60 vol% of methane, 40 vol% of carbon dioxide and a small amount of H_2S and NH_3 .^{1)–3)} Methane reforming with carbon dioxide produces hydrogen and carbon monoxide.



This reaction is expected to suppress carbon deposition from CH_4 at a high temperature. The produced H_2 and CO can be used as fuels of solid oxide fuel cell (SOFC) and react with O^{2-} ion supplied from solid electrolyte to form H_2O , CO_2 and electrons. The exhaust CO_2 is again mixed with biogas to make a closed system of $\text{CO} \rightarrow \text{CO}_2 \rightarrow \text{CO}$. That is, both methane and carbon dioxide of biogas can be used as fuels of SOFC. The above closed system of biogas is useful in producing electric power and suppresses the exhaust of CH_4 and CO_2 into air.

In our previous paper,⁴⁾ the reaction of the methane-carbon dioxide system was studied using 30 vol% $\text{Ni-Al}_2\text{O}_3$ porous compact. Methane reacted with carbon dioxide in the $\text{Ni-Al}_2\text{O}_3$ catalyst to form H_2 and CO above 400°C . As a parallel reaction, thermal decomposition of CH_4 proceeded to form H_2 and C in the temperature range from 400 to 700°C .



This carbon deposition caused the blockage of gas flow in several hours. In the lower temperature below 600°C , the formed CO decomposed to CO_2 and C .



This is another process of carbon deposition. Although CH_4

reforming with CO_2 is an attractive reaction, the above parallel reactions of carbon deposition should be prevented to maintain the smooth gas flow during the reforming of CH_4 with CO_2 .

Figure 1 shows the standard Gibbs free energy (ΔG°) for Eqs. (1)–(3) as a function of temperature (a) and fractions of CH_4 , CO_2 , H_2 and CO (b,c) for Eqs. (1) and (2). Equations (1) and (2) proceed at a higher temperature but Eq. (3) is suppressed at a high temperature. An actual chemical reaction is dominated by Gibbs free energy (ΔG) which is related to ΔG° and partial pressures of present gases. The influence of temperature judged from ΔG° is described above. Another factor is the gas composition in

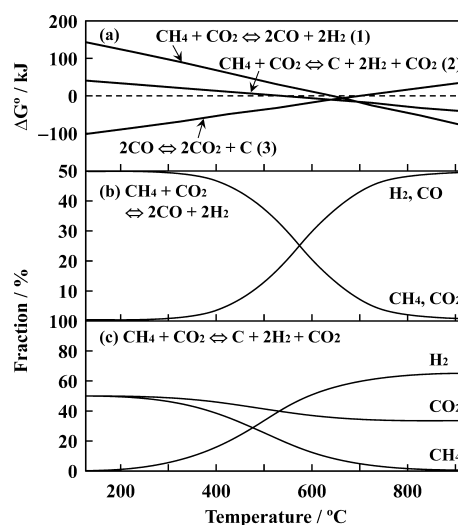


Fig. 1. Standard Gibbs free energy for Eqs. (1)–(3) as a function of temperature (a) and fractions of CH_4 , CO_2 , H_2 and CO (b, c) for Eqs. (1) and (2).

[†] Corresponding author: Y. Hirata; E-mail: hirata@apc.kagoshima-u.ac.jp

the chemical system. The composition of outlet gas can be analyzed by gas chromatography. Using these data (temperature, gas composition), the CH_4 reforming with CO_2 is discussed quantitatively. Following the previous experiment, we examined CH_4 reforming with CO_2 through a $\text{Ni-Al}_2\text{O}_3$ porous compact in a higher temperature range from 700 to 900°C. In addition, the important parallel reaction, pyrolysis of methane (Eq. (2)), was also investigated to understand the actual reaction of CH_4 reforming with CO_2 . Fortunately, it was clarified that a high temperature reaction is favorable to suppress the carbon deposition and accelerates the CH_4 reforming with CO_2 . The measured results were well understood by the corresponding thermodynamic calculation.

2. Experimental procedure

An alpha-alumina powder ($\text{Al}_2\text{O}_3 > 99.99$ mass%, median size 0.48 μm , Sumitomo Chemical Co., Ltd., Japan) was immersed into 1.4 mol/l $\text{Ni}(\text{NO}_3)_2$ solution at a volume ratio of $\text{Ni} / \text{Al}_2\text{O}_3 = 30 / 70$. The suspension was freeze-dried and then calcined at 400°C for 1 h. The calcined $\text{NiO-Al}_2\text{O}_3$ mixed powders were dispersed at 10 vol% solid in double distilled water and consolidated into a columnar shape of 16 mm diameter and 10 mm height by casting in a gypsum mold. The $\text{NiO-Al}_2\text{O}_3$ compact was calcined at 800°C for 1 h in air. The calcined $\text{NiO-Al}_2\text{O}_3$ compact with 11 mm diameter was set inside of a $\text{SiO}_2\text{-Al}_2\text{O}_3$ tube and was reduced to Ni by passing 70 vol% H_2 -30 vol% Ar gas at 800°C for 10 h.⁵⁾ Methane gas was fed at 50 ml/min at 360–1000°C. Similarly, a mixed gas of $\text{CH}_4 : \text{CO}_2 = 1 : 1$ volume ratio was fed into the $\text{Ni-Al}_2\text{O}_3$ compact at 50 ml/min at 700–900°C. A gas flow rate was measured by soap-film flow meter. Since the experiment was carried out under ambient pressure, the flow rate was not influenced by the gas pressure. The phases of $\text{Ni-Al}_2\text{O}_3$ compact before and after the reaction with CH_4 or $\text{CH}_4\text{-CO}_2$ mixed gases were identified by X-ray diffraction (RINT 2200, Rigaku Co., Tokyo, Japan). The composition of outlet gas was analyzed by gas chromatography (GT 3800, Yanaco Co., Kyoto, Japan) with activated carbon using thermal conductivity detector at 100°C to determine the reforming fractions of methane and carbon dioxide, and the amounts of formed hydrogen and carbon monoxide. The outlet gas of 0.5 ml was injected into Ar carrier gas at 100°C. The amount of carbon deposition in the $\text{Ni-Al}_2\text{O}_3$ compact was measured with thermogravimetry and differential thermal analysis (TG-DTA) at a heating rate of 10°C/min up to 1000°C in air (Thermoflex, Rigaku Co., Tokyo, Japan). Carbon is burned out as carbon dioxide and Ni is oxidized to NiO in air. The method to analyze the carbon content is reported in our previous paper.⁴⁾

3. Results

3.1 Characteristics of $\text{Ni-Al}_2\text{O}_3$ compact

No reaction between $\alpha\text{-Al}_2\text{O}_3$ and NiO was observed in the X-ray diffraction patterns of $\text{NiO-Al}_2\text{O}_3$ compact heated at 800°C. The $\text{NiO-Al}_2\text{O}_3$ compact was reduced to $\text{Ni-Al}_2\text{O}_3$ in the H_2 -rich atmosphere at 800°C and no reaction occurred between Ni and Al_2O_3 . The $\text{NiO-Al}_2\text{O}_3$ compacts heated in air contained 56% of open pores and 3% of closed pores. The open porosity increased to 63.5% and the closed pore decreased to 0.1% by the reduction of NiO to Ni with H_2 gas ($\text{NiO(s)} + \text{H}_2(\text{g}) \rightarrow \text{Ni(s)} + \text{H}_2\text{O(g)}$).

3.2 Pyrolysis of methane

Figure 2 shows the temperature dependence of pyrolysis of CH_4 in a $\text{SiO}_2\text{-Al}_2\text{O}_3$ tube. Thermal decomposition of CH_4 without $\text{Ni-Al}_2\text{O}_3$ catalyst started above 900°C. Only 15% of CH_4

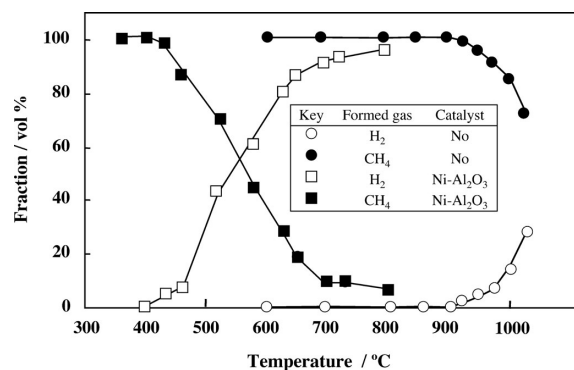


Fig. 2. Temperature dependence of pyrolysis characteristic of methane with and without $\text{Ni-Al}_2\text{O}_3$ catalyst.

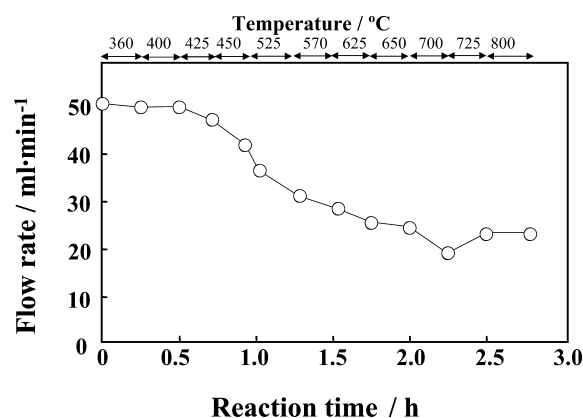


Fig. 3. Flow rate of outlet gas during the pyrolysis of CH_4 over $\text{Ni-Al}_2\text{O}_3$ catalyst at 360–800°C.

decomposed at 1000°C. As a product, formation of H_2 was recognized. The high stability of CH_4 at a high temperature results from the strong sp^3 hybrid orbital. Reduction of pyrolysis temperature is needed to use as a fuel of low temperature SOFC operated at 500–800°C. When CH_4 is passed through the $\text{Ni-Al}_2\text{O}_3$ compact, the pyrolysis temperature of CH_4 decreased to 425°C (reaction time: 0.25 h). Ni catalyst plays an important role for the decomposition of methane. It is reported that Ni catalyst promotes the dissociation of CH_4 adsorbed on Ni ($\text{CH}_4 \rightarrow \text{CH}_{1-x} + x\text{H}$) at a low temperature.⁶⁾ Figure 3 shows the flow rate of outlet gas through the $\text{Ni-Al}_2\text{O}_3$ compact during the continuous experiment of pyrolysis of methane at 360–800°C. The flow rate of CH_4 (≈ 50 ml/min) was almost independent of the reaction temperatures at 360–425°C because of little decomposition of CH_4 as shown in Fig. 2. However, the flow rate gradually decreased due to the carbon deposition in the $\text{Ni-Al}_2\text{O}_3$ compact at high temperatures. Carbon deposition over the $\text{Ni-Al}_2\text{O}_3$ compact and the inside of the $\text{SiO}_2\text{-Al}_2\text{O}_3$ tube were observed after the pyrolysis for 3 h. The amount of deposited carbon was 54.0 g / 100 g of $\text{Ni-Al}_2\text{O}_3$ catalyst $\cdot \text{h}^{-1}$. The XRD pattern of $\text{Ni-Al}_2\text{O}_3$ compact after the reaction at 800°C confirmed the formation of graphite at $2\theta = 26.6^\circ$ of diffraction angle using Cu K α . The similar carbon deposition occurred for the reforming of 50 vol% $\text{CH}_4 - 50$ vol% CO_2 system at 400–700 °C in our previous paper.⁴⁾

3.3 Reforming of methane with carbon dioxide

Figure 4 shows the flow rate of $\text{CH}_4\text{-CO}_2$ gas passed through

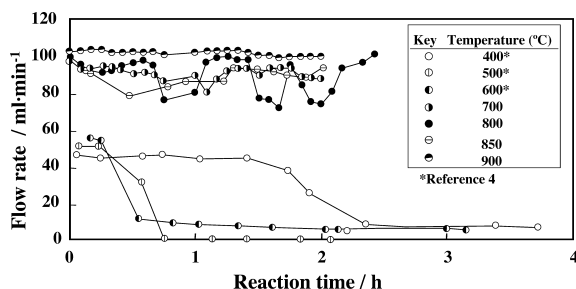


Fig. 4. Flow rate of outlet gas during the reforming of methane with carbon dioxide through Ni-Al₂O₃ compact at 400–900°C.

the Ni-Al₂O₃ compact at 700–900°C. No blockage was measured for 2 h at each reaction temperature. Furthermore, the flow rate of the outlet gas became two times (100 ml/min) larger than that of inlet gas. The above results indicate that (1) Ni in the Al₂O₃ compact promotes the reforming of methane with carbon dioxide to form hydrogen and carbon monoxide in a temperature range above 700°C, (2) this reforming is accompanied by the increase of the volume of gases (two times), and (3) carbon deposition is significantly suppressed. These results are discussed more latterly. On the other hand, Fig. 4 also shows the flow rate of outlet gas during the reactions at 400–600°C in our previous experiment.⁴⁾ The flow rate of the outlet gas decreased within 1 h at 500–600°C. In a low temperature range, the parallel reactions by Eqs. (2) and (3) are more accelerated rather than the reforming of CH₄ with CO₂ (Eq. (1)). As shown in Fig. 2, the pyrolysis of CH₄ started easily above 400°C over Ni catalyst. In the low temperature region, CO₂ is relatively stable over Ni catalyst and this stability of CO₂ inhibits the chemical reaction with CH₄ (Fig. 5).

Figure 5 shows the fractions of methane, carbon dioxide, hydrogen and carbon monoxide as a function of reaction temperature. The solid circles indicate the average fraction for 0.6–2.4 h of reforming of CH₄ where no blockage of passing gas occurred in the Ni-Al₂O₃ compact. The fraction of methane gradually decreased with increasing reaction temperature. However, CO₂ was stable at temperatures below 600°C. This behavior of CO₂ is related to the small amount of CO at 400–600°C. The pyrolysis of methane is responsible for the formation of H₂ in the low temperature range. On the other hand, decomposition of CO₂ and formation of CO became significant in the high temperature range. This result is associated with the reforming of CH₄ with CO₂ (Eq. (1)) and is supported by the smooth flow of outlet gas in Fig. 4. At a high temperature (> 700°C), carbon deposition is suppressed by the high reactivity of CO₂.

Figure 6 shows the H₂ / CO molar ratio as a function of reaction temperature. In the lower temperature range from 400 to 600°C, the average ratio was in the range from 1.9 to 2.9. In the higher temperature range, the ratio approached 1.2. This result indicates the reforming of CH₄ with CO₂ becomes a dominant reaction. After the reaction at 700–900°C, no carbon deposition was observed on the Ni-Al₂O₃ compact and inside of the SiO₂-Al₂O₃ tube. The amount of carbon deposited in the Ni-Al₂O₃ compact after the continuous experiments at 700–900°C was 0.06 g/100 g Ni-Al₂O₃ compact · h⁻¹ by TG-DTA analysis. When Eqs. (1) and (2) proceed at the same time, the molar ratio of H₂/CO gases formed (*Y*) is equal to the molar ratio of CH₄/CO₂ gases used (*X*).⁷⁾ The *Y* values measured at 700–900°C were about 1.2 (Figs. 5 and 6), indicating less consumption of CO₂ as compared with the amount of CH₄ used (*X* = 1 mol CH₄ /

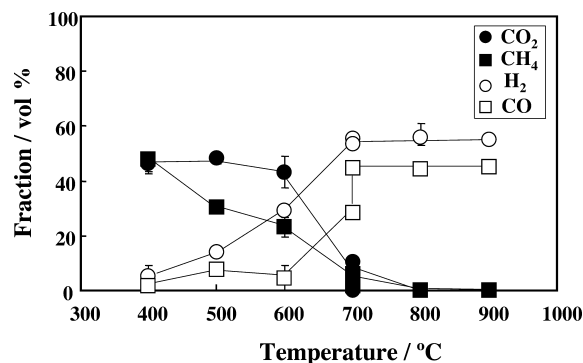


Fig. 5. Fractions of CH₄, CO₂, H₂ and CO as a function of reaction temperature in CH₄ reforming with CO₂.

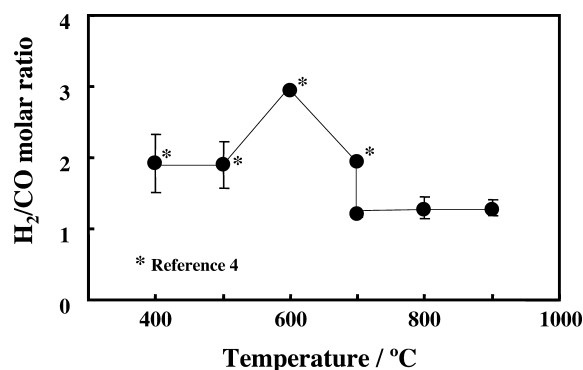


Fig. 6. H₂/CO molar ratio as a function of reaction temperature in CH₄ reforming with CO₂.

0.82 mol CO₂). However, little CO₂ was detected in the exhaust gas at 700–900°C. This reason is not clear at this moment and further investigation is needed to explain the mass balance of CO₂.

4. Discussion

4.1 Pyrolysis of methane

In the reforming of CH₄ with CO₂, pyrolysis of CH₄ occurs as a parallel reaction in the low temperature range. This parallel reaction is accompanied by the deposition of carbon in the Ni-Al₂O₃ compact and should be prevented to maintain the smooth flow of the mixed gas. Fortunately, the reforming rate of CH₄ with CO₂ becomes a dominant reaction as compared with the pyrolysis of CH₄ at a higher temperature. However, we should have the knowledge about the pyrolysis of CH₄ to suppress the carbon deposition in the Ni-Al₂O₃ compact.

The free energy for Eq. (2) is expressed by Eq. (4),

$$\Delta G(2) = \Delta G^\circ(2) + RT \ln \left(\frac{P_{\text{H}_2}^2}{P_{\text{CH}_4}} \right) \quad (4)$$

where P_{CH_4} and P_{H_2} are the partial pressures in the reaction system. Figure 7 (a) shows the fractions of inlet and outlet gases through the Ni-Al₂O₃ porous compact. The fractions of outlet gases can be analyzed by gas chromatography but it is difficult to analyze the fraction profile in the Ni-Al₂O₃ compact. In Fig. 7, a simple linear relation is drawn to understand the essence of carbon deposition in the compact. The fractions of CH₄ (A) and H₂ (D) in the Ni-Al₂O₃ compact are represented by Eqs. (5) and

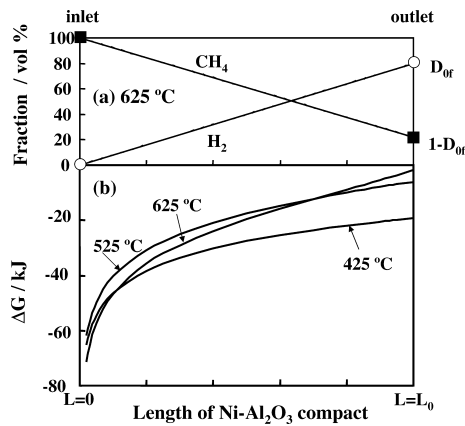


Fig. 7. Fraction profile (a) of CH_4 and H_2 along $\text{Ni-Al}_2\text{O}_3$ compact at 625°C and free energy of pyrolysis of CH_4 (b) as a function of distance from the surface of the compact at 425 – 625°C . The ΔG at 425 and 525°C was calculated using the D_{of} values measured at these temperatures.

(6) as a function of distance (L) from its surface, respectively,

$$A = 1 - \left(\frac{L}{L_0} \right) D_{\text{of}} \quad (5)$$

$$D = \left(\frac{L}{L_0} \right) D_{\text{of}} \quad (6)$$

where D_{of} is the fraction of H_2 in the outlet gas and L_0 ($= 7.6$ mm) is the thickness of $\text{Ni-Al}_2\text{O}_3$ compact. Equations (5) and (6) are substituted for P_{CH_4} and P_{H_2} in Eq. (4), respectively, because of the relation, $P_{\text{CH}_4} + P_{\text{H}_2} = 1$ atm. Equation (7) represents $\Delta G(2)$ in the $\text{Ni-Al}_2\text{O}_3$ compact as a function of distance L from the surface of the compact against the flow of CH_4 .

$$\Delta G(2) = \Delta G^\circ(2) + RT \ln \frac{(L D_{\text{of}})^2}{L_0(L_0 - L D_{\text{of}})} \quad (7)$$

Figure 7(b) shows $\Delta G(2)$ at 425 – 625°C for the measured D_{of} . The condition $L = 0$ results in $\Delta G \rightarrow -\infty$, indicating the progress of pyrolysis of methane at $L = 0$. The condition of $L = L_0$ results in $\Delta G(2) = \Delta G^\circ(2) + RT \ln [D_{\text{of}}^2 / (1 - D_{\text{of}})]$. The calculated $\Delta G(2)$ value was minus values in whole $\text{Ni-Al}_2\text{O}_3$ compact at a given temperature. This thermodynamic model explains the pyrolysis of CH_4 in the whole part of $\text{Ni-Al}_2\text{O}_3$ compact and the resultant carbon deposition, which causes the blockage of flow of CH_4 . As seen Fig. 2, D_{of} is 0 below 400°C . This condition provides $\Delta G \rightarrow -\infty$ in Eq. (7). This calculation implies that pyrolysis of methane occurs thermodynamically at 300 – 400°C but the reaction rate is very slow. As a result, no H_2 was measured at temperature below 400°C .

4.2 Reforming of CH_4 with CO_2

In the reforming of CH_4 with CO_2 (Eq. (1)), the following ΔG (1) is derived.

$$\Delta G(1) = \Delta G^\circ(1) + RT \ln \left(\frac{P_{\text{CO}_2} P_{\text{H}_2}}{P_{\text{CH}_4} P_{\text{CO}_2}} \right) \quad (8)$$

Figure 8 (a) shows the fraction profile of CH_4 (A), CO_2 (B), H_2 (D) and CO (E) in the $\text{Ni/Al}_2\text{O}_3$ compact ($L_0 = 8.8$ mm). The fraction of each gas is presented as follows,

$$A = A_0 - \left(\frac{A_0 - A_{\text{of}}}{L_0} \right) L \quad (9)$$

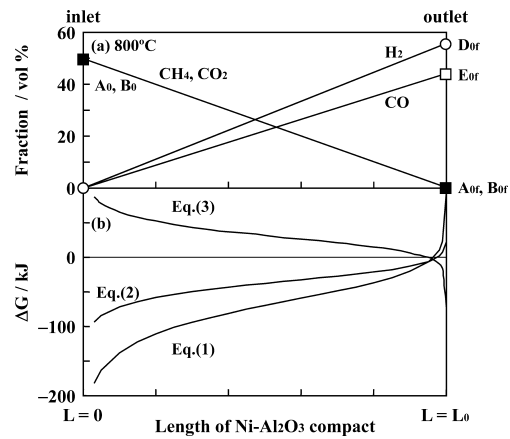


Fig. 8. Fraction profile (a) of CH_4 , CO_2 , H_2 and CO along $\text{Ni-Al}_2\text{O}_3$ compact at 800°C and free energy (b) for reforming of CH_4 with CO_2 , pyrolysis of CH_4 and decomposition of CO ($2\text{CO} \rightarrow \text{C} + \text{CO}_2$) along the distance of $\text{Ni-Al}_2\text{O}_3$ compact from the surface at 800°C .

$$B = B_0 - \left(\frac{B_0 - B_{\text{of}}}{L_0} \right) L \quad (10)$$

where A_0 and B_0 are the fractions of CH_4 and CO_2 at $L = 0$, respectively.

$$D = \left(\frac{L}{L_0} \right) D_{\text{of}} \quad (11)$$

$$E = \left(\frac{L}{L_0} \right) E_{\text{of}} \quad (12)$$

These relations are substituted for Eq. (8) to express ΔG (1) as a function of distance L (Eq. (13)).

$$\Delta G(1) = \Delta G^\circ(1) + RT \ln \left(\frac{L}{L_0} \right)^4 \frac{(E_{\text{of}} D_{\text{of}})^2 L_0^2}{[(L_0 A_0 - (A_0 - A_{\text{of}})L][(L_0 B_0 - (B_0 - B_{\text{of}})L)]} \quad (13)$$

This equation results in $\Delta G \rightarrow -\infty$ at $L = 0$ and in $\Delta G(1) = \Delta G^\circ(1) + RT \ln [(E_{\text{of}} D_{\text{of}})^2 / A_{\text{of}} B_{\text{of}}]$ at $L = L_0$. Similarly, the parallel reaction by Eq. (2) (pyrolysis of CH_4) is expressed by Eq. (14),

$$\Delta G(2) = \Delta G^\circ(2) + RT \ln \left(\frac{L}{L_0} \right)^2 \frac{D_{\text{of}}^2 L_0}{L_0 A_0 - (A_0 - A_{\text{of}}) L} \quad (14)$$

$\Delta G(2)$ approaches $-\infty$ at $L = 0$ and $\Delta G^\circ(2) + RT \ln (D_{\text{of}}^2 / A_{\text{of}})$ at $L = L_0$. The parallel reaction by Eq. (3) is expressed by Eq. (15),

$$\Delta G(3) = \Delta G^\circ(3) + RT \ln \left(\frac{L_0 B_0 - (B_0 - B_{\text{of}})L}{L_0} \right) \left(\frac{L_0}{L E_{\text{of}}} \right)^2 \quad (15)$$

$\Delta G(3)$ in Eq. (15) approaches $+\infty$ at $L = 0$ and results in $\Delta G^\circ(3) + RT \ln (B_{\text{of}} / E_{\text{of}}^2)$ at $L = L_0$.

Figure 8 (a) shows the fraction profile of CH_4 , CO_2 , H_2 and CO along $\text{Ni-Al}_2\text{O}_3$ compact. The corresponding ΔG at 800°C is shown in Fig. 8 (b). The CH_4 reforming with CO_2 proceeds in the wide range of $\text{Ni-Al}_2\text{O}_3$ compact against the flow of CH_4 – CO_2 mixed gases. Similarly $\Delta G(2)$ for pyrolysis of methane pro-

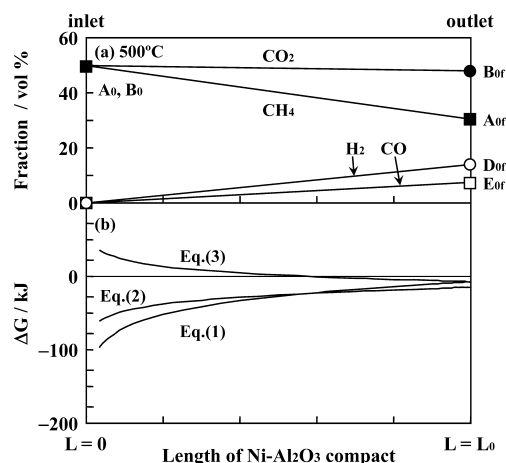


Fig. 9. Fraction profile (a) of CH₄, CO₂, H₂ and CO along Ni-Al₂O₃ compact at 500°C and free energy (b) for reforming of CH₄ with CO₂, pyrolysis of CH₄ and decomposition of CO (2CO → C + CO₂) along the distance of Ni-Al₂O₃ compact from the surface at 500°C.

ceeds in the Ni-Al₂O₃ compact. However, ΔG (3) for Eq. (3) becomes a plus value in the wide range of the Ni-Al₂O₃ compact. However, the measured amount of carbon in the Ni-Al₂O₃ compact was significantly small at 700–900°C. This result is related to the reaction rates for Eqs. (1)–(3). When ΔG is an enough minus value, the dominant reaction is controlled by the reaction rate. From the measured results, the reforming rate by Eq. (1) is far higher rather than that by Eq. (2) at 700–900°C. This is supported by the formation of CO in a high temperature range.

Figure 9 (a) shows the fraction profile of CH₄, CO₂, H₂ and CO along the Ni-Al₂O₃ compact. The ΔG values for Eqs. (1)–(3) at 500°C are shown in Fig. 9 (b). The ΔG values for Eqs. (1) and (2) became minus values in the wide range of Ni-Al₂O₃ compact. On the other hand, the ΔG value for Eq. (3) changed from a plus value to a minus value as the length of the compact increases. The thermodynamic calculation indicates that Eqs. (1)

and (2) proceed at 500°C. In fact, a large amount of carbon was formed in the low temperature range from 400 to 600°C. However the reactivity of CO₂ is very low as seen in Fig. 5. That is, Eq. (2) (pyrolysis of CH₄) is a dominant reaction at 400–600°C. As discussed above, the dominant reaction shifts to Eq. (1) (reforming of CH₄ with CO₂) in a high temperature range because of the high reactivity of CO₂, which gives a higher reaction rate rather than the pyrolysis rate of CH₄.

5. Conclusions

(1) Pyrolysis of CH₄ occurred above 900°C and only 15% of CH₄ decomposed thermally over no catalyst at 1000°C.

(2) When the mixed gas of 50% CH₄–50% CO₂ was passed through Ni-Al₂O₃ compact, pyrolysis of CH₄ (CH₄ → C + 2H₂) proceeded dominantly at 400–600°C. However, the reforming of CH₄ with CO₂ (CH₄ + CO₂ → 2H₂ + 2CO) became a dominant reaction in the higher temperature range from 700 to 900°C. As a result, no blockage of the flowing gas was measured.

(3) Thermodynamic calculation of pyrolysis of CH₄ and reforming of CH₄ with CO₂ along the length of the Ni-Al₂O₃ compact explained well the measured results.

References

- 1) Y. Lu and L. Shaefer, *J. Power Sources*, 135, 184–191 (2004).
- 2) M. Nagamori, Y. Hirata and S. Sameshima, *Mater. Sci. Forum*, 544–545, 985–988 (2007).
- 3) H. Purwanto and T. Akiyama, *Inter. J. Hydrogen Energy*, 31, 491–495 (2006).
- 4) S. Sameshima, Y. Hirata, J. Sato and N. Matsunaga, *J. Ceram. Soc. Japan*, 116, 374–379 (2008).
- 5) S. Sameshima, Y. Hirata and K. Higashinakagawa, Proceedings of 6th Pacific Rim Conference on Ceramic and Glass Technology, Am. Ceram. Soc., CDR (2006).
- 6) Y. Cui, H. Zhang, H. Xu and W. Li, *Appl. Catal. A: General*, 318, 79–88 (2007).
- 7) Y. Hirata, Y. Terasawa, N. Matsunaga and S. Sameshima, *Ceram. Int.*, online available (2009).